



## ARTICLE

# Optimal Operation Strategy of Electricity-Hydrogen Regional Energy System under Carbon-Electricity Market Trading

Jingyu Li<sup>1,2</sup>, Mushui Wang<sup>1,2,\*</sup>, Zhaoyuan Wu<sup>1,3</sup>, Guizhen Tian<sup>1,2</sup>, Na Zhang<sup>1,2</sup> and Guangchen Liu<sup>1,2</sup>

<sup>1</sup>Inner Mongolia Key Laboratory of Electrical Energy Conversion Transmission and Control, Inner Mongolia University of Technology, Hohhot, 010080, China

<sup>2</sup>School of Electric Power, Inner Mongolia University of Technology, Hohhot, 010080, China

<sup>3</sup>School of Electrical and Electronic Engineering, North China Electric Power University, Beijing, 102206, China

\*Corresponding Author: Mushui Wang. Email: wangmushui07@163.com

Received: 10 August 2023 Accepted: 19 October 2023 Published: 27 February 2024

## ABSTRACT

Given the “double carbon” objective and the drive toward low-carbon power, investigating the integration and interaction within the carbon-electricity market can enhance renewable energy utilization and facilitate energy conservation and emission reduction endeavors. However, further research is necessary to explore operational optimization methods for establishing a regional energy system using Power-to-Hydrogen (P2H) technology, focusing on participating in combined carbon-electricity market transactions. This study introduces an innovative Electro-Hydrogen Regional Energy System (EHRES) in this context. This system integrates renewable energy sources, a P2H system, cogeneration units, and energy storage devices. The core purpose of this integration is to optimize renewable energy utilization and minimize carbon emissions. This study aims to formulate an optimal operational strategy for EHRES, enabling its dynamic engagement in carbon-electricity market transactions. The initial phase entails establishing the technological framework of the electricity-hydrogen coupling system integrated with P2H. Subsequently, an analysis is conducted to examine the operational mode of EHRES as it participates in carbon-electricity market transactions. Additionally, the system scheduling model includes a stepped carbon trading price mechanism, considering the combined heat and power generation characteristics of the Hydrogen Fuel Cell (HFC). This facilitates the establishment of an optimal operational model for EHRES, aiming to minimize the overall operating cost. The simulation example illustrates that the coordinated operation of EHRES in carbon-electricity market transactions holds the potential to improve renewable energy utilization and reduce the overall system cost. This result carries significant implications for attaining advantages in both low-carbon and economic aspects.

## KEYWORDS

Regional energy system; electro-hydrogen coupling; carbon-electricity market; step carbon trading; coordination and optimization

## 1 Introduction

In recent years, with the deterioration of environmental resources and the increasing demand for energy, the efficient reduction of carbon dioxide emissions and the promotion of green and low-carbon energy sources have become hot topics in many countries worldwide [1]. During the 75th United Nations General Assembly, the Chinese government set an ambitious and forward-thinking



This work is licensed under a Creative Commons Attribution 4.0 International License, which permits unrestricted use, distribution, and reproduction in any medium, provided the original work is properly cited.

objective known as the “double carbon” target [2]. This goal aims to achieve the peak of carbon dioxide emissions by 2030 and carbon neutrality by 2060. Achieving this objective requires reducing reliance on conventional fossil fuels and transitioning towards more environmentally friendly and sustainable renewable energy sources.

Over the past decade, there has been a significant increase in the deployment of high-capacity clean energy sources in China, such as wind energy and solar power production. Projections indicate that the installed capacity of renewable energy is expected to reach 1.6 billion and 4 billion kilowatts by 2030 and 2060, respectively [3,4]. In the context of the flourishing low-carbon energy revolution, the EHRES has gained significant attention due to its coordinated planning and flexible scheduling of diverse energy systems, resulting in various complementarities [5].

However, it is also facing challenges, including the lag in grid construction and the uncertainty of renewable energy output, leading to issues related to energy absorption. Furthermore, within the framework of carbon-electricity market transactions, it is imperative to conduct an additional evaluation of the economic and environmental significance of EHRES. To address these challenges, Power-to-Hydrogen (P2H) technology can convert renewable energy sources into hydrogen, which can then be stored and used in EHRES [6]. P2H is widely regarded as a viable alternative for increasing the utilization of renewable energy, reducing carbon emissions, and improving system flexibility. Consequently, there is an urgent need for further research on the optimization approach for the operation of regional energy systems incorporating P2H technology in the context of joint carbon-electricity market transactions.

As the energy market undergoes extensive reform and the dual carbon target is proposed, significant transformations have occurred in the operational framework of the power system [7,8]. The government inaugurated China’s nationwide carbon trading market on July 16, 2021. Carbon Emissions Trading (CET) now includes the environmental impact of electricity production in market transactions, infusing market vitality into carbon emission reduction efforts. As a result, there is a growing integration between the carbon trading market and the power market. The implementation of carbon trading charges will have an impact on the revenue of power production companies. Higher carbon prices may encourage power generation companies to adopt cleaner energy and technology to promote low-carbon development. Conversely, the power generation capacity of these companies will subsequently affect their involvement in carbon emissions quotas within the carbon market.

In reference [9], authors verified that the electricity-carbon market synergy can couple unbalanced electricity and stimulate the load side to participate in the regulation response. In reference [10], the authors used China’s carbon trading pilot market as a case study to examine the impact of emission reduction on price and size. The findings indicate that a rise in the price of carbon trading and an expansion in trading volume have the potential to effectively mitigate carbon emissions. In reference [11], the promotion of the low-carbon transformation of traditional thermal power units is achieved by the integration of the electricity market and the carbon trading market. This integration involves matching the reduction of carbon emissions resulting from power production rights trading with corresponding economic costs. Based on the study’s findings, a significant correlation exists between the energy and carbon trading markets. Consequently, participating in the simultaneous trading of these two markets will exert influence on the economic functioning of the system as well as its environmental advantages. Consequently, the implementation of a scientifically devised operational strategy is necessary to enhance the flexibility of the system and facilitate the reduction of carbon emissions.

In recent years, P2H technology has provided a solution to the EHRES renewable energy consumption level by converting surplus electric energy into hydrogen energy for storage and utilization. In references [12–14], the system's flexibility in energy use is greatly increased by coupling hydrogen energy with other energy sources in the integrated energy system. In reference [15], P2H was employed as a flexible resource in the optimal allocation of independent microgrids, proving that it played an important role in lowering the economic cost of microgrids and increasing the proportion of renewable energy availability. In reference [16], a two-layer optimization framework was proposed, and the remaining renewable energy was converted into hydrogen through P2H, which effectively reduced operating costs and improved system safety. Previous studies have examined the optimal operation of EHRES with P2H technology using various planning approaches and operation strategies, and have demonstrated that P2H is a dependable scheduling resource.

Furthermore, because hydrogen has a wide range of conversion methods and a high efficiency, it may be used with other energy sources to construct an integrated energy utilization architecture powered by hydrogen energy. How to diversify and utilize high-grade hydrogen is crucial to improve the flexibility of EHRES. Based on the thermodynamic equation and the principle of physical reaction, Reference [17] proposed an optimal operation method considering the heat recovery of the hydrogen energy system, which effectively improved the flexibility of system operation. In reference [18], taking into account the features of various types of hydrogen production equipment, it was discovered that the heat storage device may be tuned to increase energy efficiency under changeable operating conditions, boosting the adaptability of the overall system. In reference [19], hydrogen storage system with HFC was considered in the proposed energy network operation optimization strategy, which can significantly reduce the bidding price of the system by considering the reliability index. In reference [20], a method of coordinating hydrogen energy storage technology with new energy vehicles was proposed, further promoting the achievement of emission reduction targets for integrated energy systems. However, the above literature usually rarely involves the study of the combined heat and power generation characteristics of HFC on the comprehensive operation benefits of EHRES, especially in the combined operation environment of carbon-electricity trading market. This combined heat and power generation characteristics can guide high-carbon emission units to consciously reduce power generation promptly, producing more obvious low-carbon effects and economic benefits.

Building upon the mentioned concerns, EHRES is anticipated to widen the scope of market development and encourage the integration of renewable energy. This integration is expected to contribute to the reduction of fossil fuel emissions and the realization of the objective of operating a low-carbon system economically. Therefore, to gauge the dual advantages resulting from the cogeneration attributes of HFC, we suggest implementing an EHRES designed to facilitate carbon-electricity market transactions. This EHRES would amalgamate diverse components including renewable energy sources, Power-to-Hydrogen (P2H) systems, Combined Heat and Power (CHP) units, gas boilers (GB), and a range of storage devices. This study puts forth three noteworthy contributions, delineated as follows:

- 1) The EHRES framework is implemented within the context of the carbon-electricity market trading environment. Surplus renewable energy is utilized for immediate hydrogen production. This hydrogen is subsequently integrated into the P2H system, facilitating a bidirectional conversion between power and hydrogen. This study investigates the operational characteristics of combined heat and power production using HFC within the framework of carbon-electricity market transactions. The primary goal is to pinpoint strategies for efficiently reducing the carbon transaction costs linked to the system. The emission of high carbon units within the system is efficiently mitigated through the application of HFC in combined heating processes. Concurrently, EHRES is involved

in hydrogen production through the utilization of electrolytic cell technology when power prices are low. Subsequently, any surplus electricity is sold. Conversely, the system employs HFC for electricity generation, thereby alleviating the necessity for external energy acquisition and diminishing related expenses.

2) The optimal operational model for EHRES is constructed based on the hierarchical carbon trading pricing mechanism, considering the interactions within the carbon-electricity market. To accommodate constraints involving square terms, the piecewise linearization technique is utilized to transform the above-mentioned model into the MIQP model. By considering the economic and low-carbon aspects of system operation, the optimal solution is determined to minimize the overall operational cost.

3) Four case studies were conducted to assess and analyze the effectiveness and rationale of the proposed model. These studies concentrate on the HFC cogeneration characteristics and the hierarchical carbon trading price mechanism. The data employed in these case studies were gathered from daily records in a specific region of Northern China. The assessment of numerous benefits obtained by EHRES through participation in carbon-electricity market transactions involves quantifying their influence on system economics, low-carbon attributes, and the rate of new energy consumption. To explore the most efficient configuration for hydrogen storage capacity within the P2H system, a sensitivity analysis of the carbon trading price mechanism is performed. Subsequently, the proposed optimization technique is validated to illustrate its superiority. The provided reference supports EHRES' engagement in carbon reduction planning and economic activities within carbon-electricity market transactions, aligning with the context of the "double carbon" objective.

## 2 Building EHRES for Carbon-Electricity Trading

### 2.1 *The Framework and Operation Principle of an Electro-Hydrogen Coupling System*

To enhance the adaptability of the electro-hydrogen coupling unit, a regional energy system using electro-hydrogen technology has been devised. The process of P2H involves the conversion of distributed solar and wind power within a regional energy system into hydrogen. This hydrogen is then used to HFC via an electrolyzer (EL). The purpose of this conversion is to satisfy the power and heat requirements within the energy system. The hydrogen that remains may be kept inside a designated Hydrogen Storage Tank (HST). [Fig. 1](#) displays the schematic diagram of the EHRES, which is constructed based on the principle of electro-hydrogen coupling.

The electricity-hydrogen regional energy system integrates P2H systems, renewable energy sources, conventional energy sources, and controllable loads to participate in carbon-electricity market transactions. In the carbon emissions trading market, this paper utilizes carbon emission quotas for carbon trading [21]. If carbon emissions from conventional units exceed their allocated quotas, additional carbon quotas must be purchased. Conversely, surplus carbon quotas can be sold to promote low-carbon operation of the system. In electricity trading markets, the hydrogen stored in HST can be used to generate electricity through HFC during periods of high electricity prices, reducing the need for external electricity purchases and associated costs.

Conversely, during periods of low electricity prices, surplus renewable energy can be converted into hydrogen using the EL. The resulting surplus electricity can then be sold, providing financial benefits [22]. This approach maximizes the potential of hydrogen energy, enhancing the efficiency, cleanliness, and flexibility of the EHRES supply.

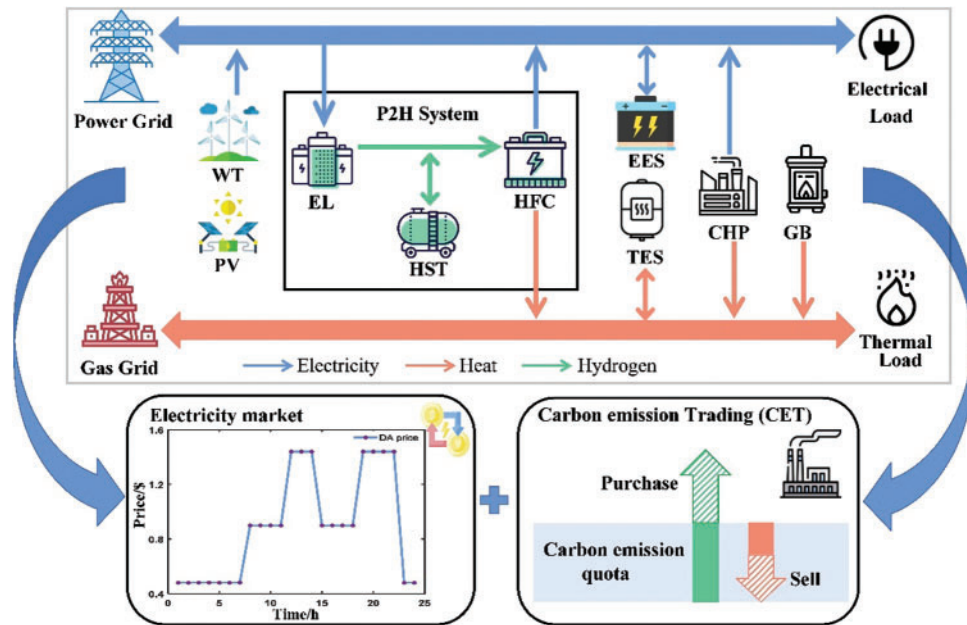


**Figure 1:** Electro-hydrogen coupling system framework

**2.2 The Operating Characteristics of HFC Cogeneration**

The combined heat and power generation attributes of HFC pertain to an operational approach that involves simultaneously providing electrical and thermal energy to end-users through fuel cell power generation technology. After the electrolytic production of hydrogen, HFC facilitates the provision of electricity to external entities through hydrogen-electricity conversion. However, it is worth noting that the power generation efficiency of this particular procedure typically ranges from around 30% to 50% [23]. Additionally, a significant portion of the energy is dissipated in the form of heat energy. HFC can effectively harness this particular energy segment through the utilization of hydrogen for cogeneration. This approach offers notable benefits, including enhanced energy utilization efficiency and reduced carbon emissions. Fig. 2 illustrates the utilization mode of HFC cogeneration features.

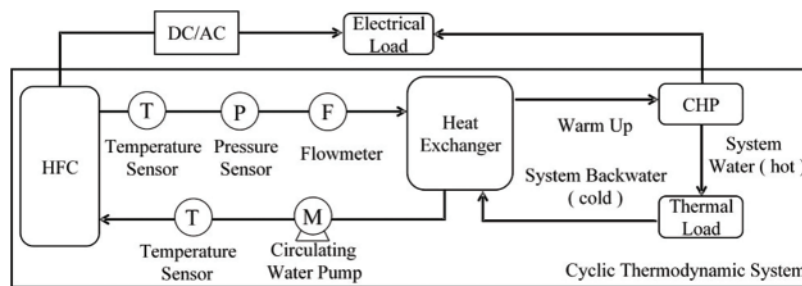


**Figure 2:** HFC cogeneration utilization mode

Fig. 2 illustrates that the circulating thermal system primarily employs the heat exchanger as a medium for facilitating the passage of thermal energy between the heating pipeline and the regenerating pipeline [24]. The transmission of electric power to the power grid mostly occurs via



reduction efforts [26]. Currently, the carbon emission trading pricing mechanism in China can be categorized into two types: fixed carbon trading prices and tiered carbon trading prices. Carbon quotas are initially allocated at no cost, and the initial free carbon quota is obtained through the baseline method allocation.

In this paper, the carbon emission sources within EHRES include external power grid purchases, CHP units and GB; the external power grid purchase is associated with the power generation from coal-fired units. The carbon emission quota  $E_a(t)$  and the total carbon emissions  $E_{co_2}(t)$  of the system at time  $t$  can be expressed as follows:

$$E_a(t) = \delta_c P_t^{buy} + \delta_g (G_t^{CHP} + G_t^{GB}) \tag{1}$$

$$E_{co_2}(t) = a_{CHP} (C_{v1} Q_t^{CHP} + P_t^{CHP})^2 + b_{CHP} (C_{v1} Q_t^{CHP} + P_t^{CHP}) + c_{CHP} + \lambda_{GB} Q_t^{GB} + \lambda_{buy} P_t^{buy} \tag{2}$$

where  $\delta_c$  is the carbon emission factor of unit external power grid purchase, kW·h;  $\delta_g$  is the carbon emission quota factor of natural gas consumption units [27], kW·h.  $G_t^{CHP}$  and  $G_t^{GB}$  represent the natural gas consumption power of CHP and GB at time  $t$ , m<sup>3</sup>.  $P_t^{buy}$  represents the quantity of energy acquired from an external power grid at the time instance  $t$ , kW;  $a_{CHP}$ ,  $b_{CHP}$ , and  $c_{CHP}$  are the unit carbon emission coefficients of CHP, kg/kWh;  $\lambda_{GB}$  is the unit carbon emission coefficient of GB, kg/kWh.  $\lambda_{buy}$  is the carbon emission coefficient per unit of electricity for coal-fired units.

From this, it is evident that carbon quota trading assigns environmental value to carbon, thereby enhancing the integration of the electricity-hydrogen energy system and enabling adjustments to its production plan to achieve a more effective reduction of carbon emissions while maintaining a balance between energy supply and demand.

Within the carbon trading market, the conventional cost associated with carbon transactions is denoted as  $F_{co_2}$ .

$$F_{co_2} = p_{co_2}^0 (E_{co_2} - E_a) \tag{3}$$

where  $P_{co_2}^0$  represents the starting price of carbon trading units, \$/t.

The reasonableness of carbon trading prices significantly influences the effectiveness of emission reduction measures. The traditional carbon trading mechanism, with its fixed carbon trading price, has limitations in fully exploring opportunities for energy savings and carbon reduction. Implementing a tiered pricing system represents a strategic approach in the market. This approach seeks to allocate carbon emission rights by categorizing them into intervals based on market factors, thereby facilitating efficient management. Unlike the conventional carbon trading mechanism, the stepped carbon trading mechanism can enhance the efficient utilization of energy and amplify the impact of energy conservation and emission reduction initiatives.

$$p_{co_2} = \begin{cases} -p_{co_2}^0 & -l \leq E_{co_2} - E_a < 0 \\ p_{co_2}^0 & 0 \leq E_{co_2} - E_a < l \\ (1 + \alpha)p_{co_2}^0 & l \leq E_{co_2} - E_a < 2l \\ \dots & \dots \\ (1 + N\alpha)p_{co_2}^0 & E_{co_2} - E_a \geq Nl \end{cases} \tag{4}$$

where  $\alpha$  represents the coefficient of carbon price rise,  $N$  denotes the quantity of intervals for carbon emissions, and  $l$  signifies the duration of each interval, kg. Accordingly, based on the ladder pricing mechanism, the cost of the system carbon trading market is denoted as  $F_{co_2}$ :

$$F_{co_2} = p_{co_2} (E_{co_2} - E_a) \tag{5}$$

### 3 Optimal Operation Strategy of Energy System with Electricity-Hydrogen Coupling

#### 3.1 Mathematical Model of EHRES

##### 1) Electric hydrogen production link

The EL serves as a crucial apparatus in electrolyzing water to generate hydrogen. It facilitates the conversion of electrical energy into hydrogen energy, hence playing a pivotal role in integrating the electro-hydrogen system. Its related expressions are as follows:

$$H_t^{\text{EL}} = \frac{P_t^{\text{EL}} \cdot \eta_{\text{EL}}}{L_{\text{H}_2}} \cdot \Delta t \quad (6)$$

$$P_{\min}^{\text{EL}} \leq P_t^{\text{EL}} \leq P_{\max}^{\text{EL}} \quad (7)$$

$$\Delta P_{\min}^{\text{EL}} \leq P_t^{\text{EL}} - P_{t-1}^{\text{EL}} \leq \Delta P_{\max}^{\text{EL}} \quad (8)$$

where  $H_t^{\text{EL}}$  is the power associated with hydrogen generation at a certain time  $t$ ,  $\text{m}^3$ ;  $P_t^{\text{EL}}$  is the power consumption in EL, kW;  $\eta_{\text{EL}}$  represents the energy conversion efficiency of the hydrogen production process;  $P_{\min}^{\text{EL}}$  and  $P_{\max}^{\text{EL}}$  denote the boundary values of the input power for EL, respectively, kW;  $\Delta P_{\min}^{\text{EL}}$  and  $\Delta P_{\max}^{\text{EL}}$  denote the upper and lower boundaries of the EL ramp value, respectively, kW/h;  $L_{\text{H}_2}$  is the low calorific value of hydrogen,  $\text{kWh}/\text{m}^3$ .

##### 2) HFC cogeneration link

HFC is an important energy coupling device in EHRES. Due to voltage loss, some energy is dissipated as thermal energy. Considering the characteristics of cogeneration of HFC, The related expressions are as follows [18]:

$$\begin{cases} P_t^{\text{HFC}} = \frac{2Fv_{\text{H}_2,t}}{M_{\text{H}_2}}(E_{\text{ner}} - V_{\text{act}} - V_{\text{ohm}} - V_{\text{con}}) \\ Q_t^{\text{HFC}} = \frac{2Fv_{\text{H}_2,t}}{M_{\text{H}_2}}(V_{\text{act}} + V_{\text{ohm}} + V_{\text{con}}) \\ E_{\text{ner}} = 1.299 - \frac{\Delta S(T_R - 298)}{2F} + \frac{R_a T_R \ln(P_{\text{H}_2} P_{\text{O}_2}^{1/2})}{2F} \\ V_{\text{act}} = k_1 + k_2 T_R + k_3 T_R \ln \left[ \frac{P_{\text{O}_2}}{5.08 \times 10^6 \exp(-498/T_R)} \right] + k_4 T_R \ln i \\ V_{\text{ohm}} = iR_i \\ V_{\text{con}} = \lambda \exp(ni) \end{cases} \quad (9)$$

where  $P_t^{\text{HFC}}$  and  $Q_t^{\text{HFC}}$  represent the power and heat generation power, kW;  $E_{\text{ner}}$ ,  $V_{\text{act}}$ ,  $V_{\text{ohm}}$  and  $V_{\text{con}}$  are the Nernst voltage; activation loss voltage, ohmic overpotential and concentration over-voltage loss;  $v_{\text{H}_2}$  represents the input hydrogen supply rate, kg/s;  $F$  is the Faraday constant, C/mol;  $\Delta S$  is the entropy change value corresponding to standard atmospheric pressure, J/(mol·K);  $T_R$  is the stack temperature, K;  $P_{\text{H}_2}$  and  $P_{\text{O}_2}$  are the partial pressures of hydrogen and oxygen, respectively, Pa;  $R_a$  is the gas constant, J/(mol·K);  $i$  represents the current density of the battery, A/cm<sup>2</sup>;  $k_1, k_2, k_3, k_4$  are empirical parameters;  $\lambda$  and  $n$  are related mass transfer coefficients;  $R_i$  represents the internal battery impedance,  $\Omega \cdot \text{cm}^2$ .

### 3.2 Objective Function

This section outlines an optimal operating strategy for EHRES, taking into account the unique characteristics of HFC cogeneration within the framework of carbon-electricity market transactions. A comprehensive explanation of the stepwise carbon trading price mechanism is presented. The primary optimization goal is to minimize the overall operational expenses of the system. These expenses comprise various components, such as the system's operational costs, the costs associated with participation in the carbon trading market, the revenue generated from power sales in the energy market, and the penalties for unused wind and solar energy.

$$\min F = F_{\text{op}} + F_e + F_{\text{co}_2} + F_{\text{cur}} + F_{\text{sto}} \quad (11)$$

$$\begin{cases} F_{\text{op}} = \sum_{t=1}^T \left[ C_{\text{WT}} P_t^{\text{W}} + C_{\text{PV}} P_t^{\text{PV}} + \alpha_1 (C_{\text{v1}} Q_t^{\text{CHP}} + P_t^{\text{CHP}})^2 + b_1 (C_{\text{v1}} Q_t^{\text{CHP}} + P_t^{\text{CHP}}) + c_1 \right] \\ \quad + C_{\text{GB}} Q_t^{\text{GB}} + C_{\text{EL}} P_t^{\text{EL}} + C_{\text{HFC}} P_t^{\text{FC}} + \sum_{i=1}^N C_{\text{sto}}^i (P_{\text{cha},t}^i + P_{\text{dis},t}^i) \\ F_e = \sum_{t=1}^T (p_e^{\text{b}} P_t^{\text{buy}} - p_e^{\text{s}} P_t^{\text{sell}}) \\ F_{\text{cur}} = c \sum_{t=1}^T [(P_{\text{max}}^{\text{W}} - P_t^{\text{W}}) + (P_{\text{max}}^{\text{PV}} - P_t^{\text{PV}})] \end{cases} \quad (12)$$

where  $F_{\text{op}}$  is the system operating costs, \$;  $F_e$  is the transaction income of the electricity market, \$;  $F_{\text{cur}}$  is the penalty costs for abandoning energy, \$;  $C_{\text{WT}}$ ,  $C_{\text{PV}}$ ,  $C_{\text{EL}}$ ,  $C_{\text{HFC}}$  and  $C_{\text{GB}}$  represent the operational expense coefficients of related equipment, \$/kW;  $C_{\text{sto}}^i$  is the operating cost of different energy storage equipment, \$/kWh  $\alpha_1$ ,  $b_1$ , and  $c_1$  are the running cost parameters of unit CHP;  $P_t^{\text{sell}}$  represents the power sold to the external grid, kW;  $P_e^{\text{b}}$  and  $P_e^{\text{s}}$  represent the relative price, \$/kWh;  $c$  represents the penalty coefficient for wind and solar power abandonment, \$/kWh.

### 3.3 Constraints

#### 1) Energy balance constraint

The restrictions that must be satisfied are the electrical, thermal, and hydrogen power balances.

$$\begin{cases} P_t^{\text{L}} + P_t^{\text{EL}} + P_{\text{cha},t}^{\text{EES}} + P_t^{\text{sell}} = P_t^{\text{W}} + P_t^{\text{PV}} + P_{\text{dis},t}^{\text{EES}} + P_t^{\text{CHP}} + P_t^{\text{HFC}} + P_t^{\text{buy}} \\ Q_t^{\text{L}} + P_{\text{cha},t}^{\text{TES}} = Q_t^{\text{CHP}} + Q_t^{\text{HFC}} + Q_t^{\text{GB}} + P_{\text{dis},t}^{\text{TES}} \\ H_t^{\text{EL}} + P_{\text{dis},t}^{\text{HST}} = H_t^{\text{HFC}} + P_{\text{dis},t}^{\text{HST}} \end{cases} \quad (13)$$

where  $P_t^{\text{L}}$  and  $Q_t^{\text{L}}$  represent the electrical and thermal loads, kW;  $P_t^{\text{W}}$  and  $P_t^{\text{PV}}$  denote the wind power and photovoltaic power available at a given moment  $t$ , kW.

#### 2) Cogeneration unit model

The CHP unit needs to meet the relevant electric output constraints and heat output constraints. The expression and related constraints are as follows:

$$\begin{cases} P_t^{\text{CHP}} \geq \max \{ P_{\text{min}}^{\text{CHP}} - C_{\text{v1}} Q_t^{\text{CHP}}, C_{\text{m}} (Q_t^{\text{CHP}} - Q_{\text{max}}^{\text{CHP}}) + P_{\text{max}}^{\text{CHP}} - C_{\text{v2}} Q_{\text{max}}^{\text{CHP}} \} \\ P_t^{\text{CHP}} \leq P_{\text{max}}^{\text{CHP}} - C_{\text{v2}} Q_t^{\text{CHP}} \end{cases} \quad (14)$$

$$Q_{\text{min}}^{\text{CHP}} \leq Q_t^{\text{CHP}} \leq Q_{\text{max}}^{\text{CHP}} \quad (15)$$

where  $P_t^{\text{CHP}}$  and  $Q_t^{\text{CHP}}$  represent the electric power and thermal power generated by the CHP unit in period  $t$ , kW;  $C_{v1}$ ,  $C_{v2}$ , and  $C_m$  represent the slope coefficients of CHP unit, respectively;  $Q_{\min}^{\text{CHP}}$  and  $Q_{\max}^{\text{CHP}}$  are the boundary values of heat production for CHP unit, kW.

### 3) HFC cogeneration link

$$\begin{cases} P_t^{\text{HFC}} + Q_t^{\text{HFC}} = \eta_{\text{HFC}} H_t^{\text{HFC}} \\ H_{\min}^{\text{HFC}} \leq H_t^{\text{HFC}} \leq H_{\max}^{\text{HFC}} \\ \Delta H_{\min}^{\text{HFC}} \leq H_t^{\text{HFC}} - H_{t-1}^{\text{HFC}} \leq \Delta H_{\max}^{\text{HFC}} \\ \tau_{\min}^{\text{HFC}} \leq Q_t^{\text{HFC}} / P_t^{\text{HFC}} \leq \tau_{\max}^{\text{HFC}} \end{cases} \quad (16)$$

where  $H_t^{\text{HFC}}$  is the hydrogen consumption power of HFC at time  $t$ , kW.  $\eta_{\text{HFC}}$  is the energy conversion efficiency of HFC;  $H_{\min}^{\text{HFC}}$  and  $H_{\max}^{\text{HFC}}$  are the boundary range of hydrogen power of HFC, kW;  $\Delta H_{\min}^{\text{HFC}}$  and  $\Delta H_{\max}^{\text{HFC}}$  represent the HFC climbing limit values, kW/h;  $\tau_{\min}^{\text{HFC}}$  and  $\tau_{\max}^{\text{HFC}}$  are the limit value of the thermoelectric ratio adjustment range of HFC.

### 4) Gas boiler model

The process of heat energy generation in GB involves the combustion of natural gas, and the subsequent expressions are as follows:

$$\begin{cases} Q_t^{\text{GB}} = \eta_{\text{h}}^{\text{GB}} G_t^{\text{GB}} H_{\text{g}} \\ \Delta Q_{\min}^{\text{GB}} \leq Q_t^{\text{GB}} - Q_{t-1}^{\text{GB}} \leq \Delta Q_{\max}^{\text{GB}} \\ Q_{\text{g},\min}^{\text{GB}} \leq Q_{\text{g},t}^{\text{GB}} \leq Q_{\text{g},\max}^{\text{GB}} \end{cases} \quad (17)$$

where  $Q_t^{\text{GB}}$  represents the heat power outputs of GB, kW;  $G_t^{\text{GB}}$  is the gas consumption power of GB,  $\text{m}^3$ ;  $Q_{\max}^{\text{GBg}}$  is the boundary value of GB gas consumption power; kW;  $\eta_{\text{h}}^{\text{GB}}$  is GB thermal efficiency;  $H_{\text{g}}$  is the low calorific value of natural gas combustion, kWh/ $\text{m}^3$ ;  $\Delta Q_{\min}^{\text{GB}}$  and  $\Delta Q_{\max}^{\text{GB}}$  represent the GB climbing limit values, kW/h.

### 5) Energy storage equipment model

This study employs a generalized mathematical model to analyze energy storage equipment in three distinct forms: electrical energy storage (EST), thermal energy storage (TES), and hydrogen energy storage, taking into account the similarities in operating performance and characteristic parameters of the same type of energy storage equipment [28,29], among them, hydrogen energy storage adopts the form of hydrogen storage tank (HST). The pertinent operational limitations are outlined as follows:

$$\begin{cases} E_t^i = (1 - \delta_i) E_{t-1}^i + \left( P_{\text{cha},t}^i \eta_{\text{cha}}^i + \frac{P_{\text{dis},t}^i}{\eta_{\text{dis}}^i} \right) \\ 0 \leq P_{\text{cha},t}^i \leq P_{\text{cha},t}^i \alpha_{\text{cha},t}^i \\ 0 \leq P_{\text{dis},t}^i \leq P_{\text{dis},t}^i \alpha_{\text{dis},t}^i \\ E_{\min}^i \leq E_t^i \leq E_{\max}^i \\ \alpha_{\text{cha},t}^i + \alpha_{\text{dis},t}^i \leq 1 \\ E_1^i = E_{24}^i \end{cases} \quad (18)$$

where  $i$  denotes the category of energy storage apparatus, including equipment such as EES, TES, and HST.  $E_t^i$  represents the energy storage capacity;  $\eta_{\text{cha}}^i$  and  $\eta_{\text{dis}}^i$  are the charging and discharging efficiency,  $P_{\text{cha}}^i$  and  $P_{\text{dis}}^i$  are the charging and discharging power, kW;  $P_{\min}^i$  and  $P_{\max}^i$  are the maximum values

of charging and discharging power, respectively, kW;  $E_{\min}^i$  and  $E_{\max}^i$  denote the boundary values of energy storage capacity, kWh;  $\alpha_{\text{cha},t}^i$  and  $\alpha_{\text{dis},t}^i$  represent the charging and discharging power state flags, respectively;  $\delta_i$  is the energy self-loss coefficient;  $E_1^i$  and  $E_{24}^i$  are the capacity stored at the beginning and end of the period, kWh.

#### 6) Wind and solar output constraints

Due to unpredictability and network transmission capacity, the system cannot absorb all new energy production. Wind power and photovoltaics scheduling must be within the predicted range to ensure reliability. Here are the precise boundaries:

$$\begin{cases} 0 \leq P_t^W \leq P_{\max}^W \\ 0 \leq P_t^{\text{PV}} \leq P_{\max}^{\text{PV}} \end{cases} \quad (19)$$

where  $P_{\max}^W$  and  $P_{\max}^{\text{PV}}$  are the expected amounts of wind energy and solar electricity, kW.

To summarize, the EHRES coordinated operation model with the P2H system is characterized by its objective function and associated restrictions. This model falls under the category of nonlinear mixed integer models. The cogeneration unit's secondary generation cost function and the piecewise function in the stepped carbon trading model, which participates in the carbon market, undergo a piecewise linearization method. This transformation allows the model to be converted into a mixed integer linear programming problem, facilitating an efficient solution. The CPLEX solver is employed in the MATLAB environment to quickly and accurately resolve the model.

## 4 Simulation Results and Discussions

### 4.1 Basic Parameter Settings

To substantiate the effectiveness of the proposed optimal operation method, this study conducts an illustrative analysis on the operation of various resources within the EHRES framework, specifically within the context of a carbon-electricity joint market trading environment. The system adopts a scheduling cycle of 24 h with 1 h as the unit scheduling period for simulation purposes. The current study focuses on selecting daily data that represents typical conditions in a specific region of North China. Fig. 4 illustrates the power curves for wind, solar, and load predictions within the EHRES on a typical daily basis. The operational and maintenance costs of each unit within the system and the associated parameters are sourced from reference [30]. Information regarding the characteristics of energy coupling equipment, energy storage equipment, and market time-of-use power prices primarily comes from existing references [31,32]. In the context of the electric hydrogen regional energy system, the penalty cost associated with the abandonment of wind and solar power units is 0.1 (\$/kWh). The initial carbon trading price is 90 (\$/t), with a price growth coefficient of 0.2. Additionally, the carbon emission interval spans 1000 kg. The relevant parameters in the electricity-hydrogen regional energy system model are summarized in Table 1.

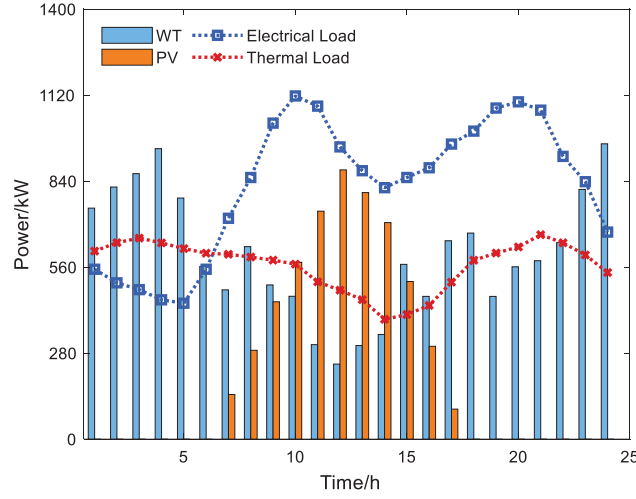


**Figure 4:** The predicted value of each load and new energy output

**Table 1:** Main parameters of system mode

Parameters	Values	Parameters	Values
$\delta_e$ (kWh)	0.78	$C_{WT}$ (\$/kW)	0.096
$\delta_g$ (kWh)	0.39	$C_{PV}$ (\$/kW)	0.096
$a_{CHP}, b_{CHP}, c_{CHP}$ (kg/kWh)	3, 0.04, 0.01	$C_{EL}$ (\$/kW)	0.547
$\lambda_{GB}$ (kg/kWh)	0.065	$C_{HFC}$ (\$/kW)	0.1825
$\lambda_{buy}$ (kg/kWh)	1.08	$C_{GB}$ (\$/kW)	0.0876
$P_{co_2}^0$ (\$/t)	90	$C_{sto}^{EES}, C_{sto}^{TES}, C_{sto}^{HST}$ (\$/kWh)	0.066, 0.12, 0.13
$\alpha$	0.2	$a_1, b_1, c_1$	0.004, 13.29, 22
$l$ (kg)	1000	$C_{v1}, C_{v2}, C_m$	0.15, 0.15, 0.75
$\eta_{EL}$	0.86	$H_g$ (kWh/m <sup>3</sup> )	9.7
$\eta_h^{GB}$	0.95	$c$ (\$/kW·h)	0.1
$\eta_{HFC}$	0.92	$E_{sto}^{EES}$ (kWh)	550
$L_{H2}$ (kWh/kg)	33.3	$E_{sto}^{TES}$ (kWh)	500
$F$ (C/mol)	96485.33	$E_{sto}^{HST}$ (kWh)	450
$T_R$ (K)	298.15	$\eta_{cha}^i, \eta_{dis}^i$	0.95
$R_a$ J/(mol·K)	8.314	$\delta_i$	0.002

## 4.2 Analysis of Scheduling Results of Electro-Hydrogen Coupling System

### 4.2.1 Economic Benefit Analysis of Electro-Hydrogen Coupling System

To analyze the economic advantages and flexibility potential of the proposed electricity-hydrogen regional energy system, considering the specific characteristics of HFC cogeneration, enhancements in wind and solar energy integration, economic management, and reduced carbon emissions within the carbon-electricity market context, we have established four scenarios for comparative evaluation

during the day-ahead phase. All four cases participate in the electricity market, but the differences are as follows:

Case 1: This scenario employs the traditional electric-thermal optimal scheduling model and does not participate in the carbon trading market.

Case 2: Building upon case 1, this scenario introduces the P2H system to achieve electricity and hydrogen coupling, considering the characteristics of HFC cogeneration. It represents the EHRES scenario but still does not participate in the carbon trading market.

Case 3: In this scenario, EHRES actively engages in the carbon-electricity joint trading market, where carbon trading adopts a unified pricing mechanism.

Case 4: Similar to case 3, EHRES participates in the carbon-electricity joint trading market, but in this scenario, the carbon trading market implements a tiered pricing mechanism (aligning with the optimal operation strategy proposed in this paper).

Table 2 shows the different settings of the four typical cases, and the optimization results under different cases are shown in Table 3.

**Table 2:** Four typical case settings

Typical case	Consider HFC cogeneration	Consider participating in the electricity trading market	Consider traditional fixed carbon pricing transactions	Consider ladder-type carbon pricing transactions
1	×	✓	×	×
2	✓	✓	×	×
3	✓	✓	✓	×
4	✓	✓	×	✓

**Table 3:** Optimization results of different cases

Case	Operation and maintenance cost	Electricity market revenue	Carbon transaction cost	New energy consumption rate /%	Total cost
1	\$653.7	\$-135.5	\$0	85.72%	\$7199.3
2	\$950.2	\$-179.0	\$0	94.68%	\$6601.6
3	\$721.7	\$-829.4	\$223.8	97.23%	\$6208.6
4	\$704.4	\$-118.5	\$282.4	99.52%	\$5951.6

As seen from the data presented in Table 3, case 2 incorporates the P2H system to achieve the integration of energy and hydrogen, in contrast to the traditional electric-thermal optimal scheduling model. With distributed photovoltaic and wind power of the regional energy system itself, renewable energy is used for localized hydrogen production by EL. The resulting hydrogen is subsequently utilized for HFC applications and stored in HST, completing the electricity-hydrogen-electricity and electricity-hydrogen-heat two-stage supply, promoting renewable energy consumption. As a result, the abandonment rate of wind and solar energy in case 2 decreased by 8.96%, leading to a significant reduction in the energy abandonment penalty incurred by the system. Additionally, in the context of

the electricity market, the EHRES system optimizes its power generation schedule based on electricity price signals. It utilizes electrolytic cells to produce hydrogen during low electricity prices, which can be sold for profit. Conversely, the HFC power generation process is scheduled during high electricity prices, effectively reducing the need for external power purchases and lowering costs. This procedure effectively utilizes the potential of the P2H system, resulting in case 2 achieving a significantly greater profit margin in the power market transaction compared to case 1, with a difference of 24.3%.

In contrast to case 2, case 3 incorporates the carbon emission trading market with a stepwise carbon price, resulting in a reduction in carbon trading costs. Currently, there is a decrease in the revenue generated by the power market, although the carbon emissions are observed to be 15.38% lower compared to scheme 2. On the whole, the overall operating cost of the system experiences a reduction exceeding 5.9%. The carbon-electricity joint market transaction involves the determination of the optimal trade-off between the two markets, with the final decision being made by EHRES. Upon careful examination of the transaction costs associated with carbon emissions, it has been seen that the environmental advantages of EHRES have been significantly enhanced. This suggests that engaging in the market for trading carbon emissions and power can lead to improved economic benefits and a reduction in operational expenses for the system.

When comparing case 4 and case 3, it becomes evident that case 4 incorporates ladder carbon pricing into the carbon-electricity joint market transaction, thereby enhancing the utilization of new energy and mitigating carbon emissions. This stands in contrast to the unified carbon pricing mechanism employed in the carbon trading market. The proposed tiered carbon trading price structure demonstrates a greater capacity for decreasing system carbon emissions, as seen by a 7.74% reduction compared to case 3. In addition, under the carbon-electricity joint market transaction considering the tiered carbon pricing mechanism, EHRES needs to consider both electricity price and carbon price, so as to allocate the limited power generation capacity reasonably in different periods according to its own operating conditions and price signals, so as to accept more renewable energy power generation proportion to make profits in the electricity market transaction, so the electricity market transaction profit increases by 13.4%.

In conclusion, it can be observed that the overall cost of case 4 is significantly reduced in comparison to the other schemes. This demonstrates that EHRES, when considering the attributes of HFC cogeneration and stepwise carbon pricing, outperforms alternative schemes in the carbon-electricity trading market regarding economic efficiency and low carbon emissions.

#### *4.2.2 The Effects of Carbon Trading Parameters on System Operation Outcomes*

Establishing an effective carbon trading mechanism is of utmost importance in the carbon-electricity coupling trading market, as it plays a vital role in enhancing the economic aspects of energy supply and facilitating the advancement of low-carbon clean energy networks. To assess the efficacy of the ladder carbon trading mechanism proposed in this study, the present investigation concentrates on analyzing the influence of key factors, namely the carbon trading unit price, carbon price growth coefficient  $\alpha$ , and carbon emission interval length  $l$ , on the operational outcomes of the EHRES. Fig. 5 illustrates the effects of fluctuations in unit carbon trading prices on the overall carbon emissions within the system across the three different cases.

Case 2's carbon emissions are unaffected by unit carbon trading price variations since the optimization model excludes the carbon emissions trading market. A negative association exists between carbon emissions and the unit carbon trading price in situations 3 and 4. The carbon emissions of case 4 are continuously lower than those of example 3. This observation supports the notion that the

stepped carbon trading mechanism is more effective than the traditional one for lowering emissions and is more conducive to reducing system emissions.

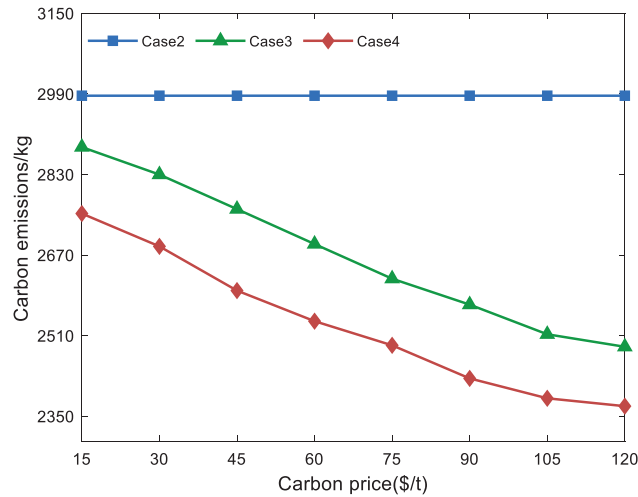


**Figure 5:** The impact of carbon trading prices on carbon emissions

Fig. 6 illustrates a negative correlation between variable  $\alpha$  and EHRES carbon emissions, while variable  $l$  exhibits a positive correlation with EHRES carbon emissions. When  $\alpha$  increases by 40% and  $l$  decreases by 40%, EHRES carbon emissions decrease by 14.7%; when  $\alpha$  is 40% and  $l$  changes from 20% to 40%, the carbon emission tends to be stable. The analysis reveals that compared with  $l$ , the change of  $\alpha$  has a greater impact on the carbon emission of EHRES. Therefore, within the current low-carbon context, it is imperative to thoroughly assess the various parameters that impact the tiered pricing system, focusing on the length of the carbon emission period. Which can greatly improve the effectiveness of reducing emissions.

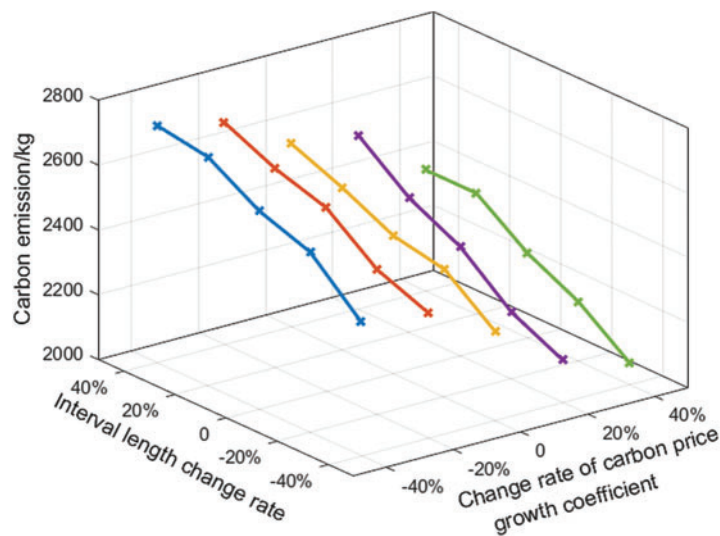
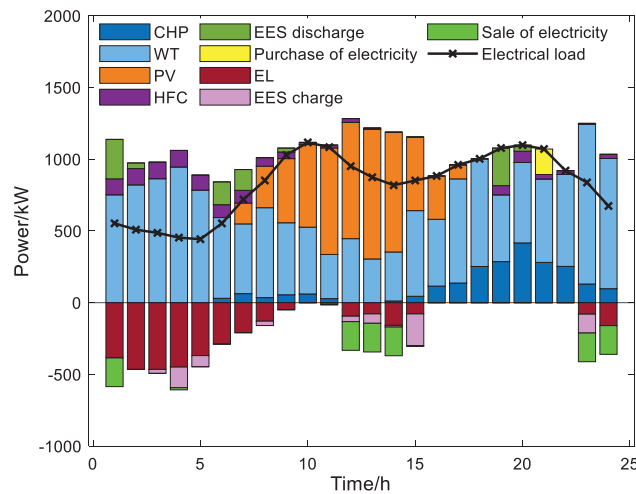


**Figure 6:** The relationship between carbon sensitive factors and system carbon emissions

#### 4.2.3 Electricity-Heat-Hydrogen Scheduling Analysis

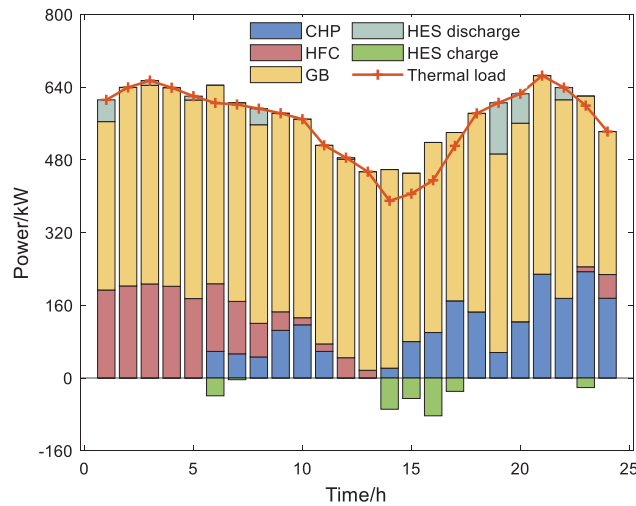
Using case 4 as a specific instance, this section provides a more in-depth examination of the optimization outcomes pertaining to the electricity, heat, and hydrogen operations of EHRES within the context of its involvement in carbon-electricity market transactions, taking into account the distinctive features of HFC cogeneration.

Fig. 7 illustrates that during the time interval from 1:00 to 5:00 in the nocturnal period, case 4 effectively achieves electric-hydrogen coupling by implementing the P2H system. This integration of additional clean energy production into the P2H system results in a notable rise of 9.46% in wind and solar energy consumption. The peak value of the system's electric load occurs between the hours of 7:00 and 10:00. The CHP unit and the wind energy are now employed to supply the electric load demand because the all-in cost of acquiring electricity from the power grid is higher than the operation cost of the gas turbine. But the CHP has a power limit. Thus, the shortfall must be filled by the EES and the HFC.



**Figure 7:** Electric load operation optimization of the case 4

The efficacy of HFC cogeneration is predominantly demonstrated in the provision of heat load, as depicted in Fig. 8. During peak heat load at 0:00–5:00 and low power load, EL effectively absorbs a significant amount of wind power to provide an energy supply for HFC cogeneration. When combined with GB to lower CHP units' heat production, HFC preferentially releases heat energy to satisfy the heat demand. At the same time, GB runs at a relatively stable heat output level throughout the day, ensuring the reliable supply of heat energy and promoting the consumption space of wind power. During the 11:00–16:00 period, the heat load demand is low at this stage. The heat storage equipment stores surplus heat energy and releases it at 19:00–21:00. GB also maintains a steady heat production throughout the day, offering a reliable heat supply and increasing wind power use. Between 11:00 and 16:00, heat load demand is low. For heat load reliability, heat storage equipment discharges surplus heat energy at 19:00–21:00. Though GB has better thermal efficiency than the CHP unit, the current electrical load is quite large, and wind power generation is relatively low. Therefore, the CHP unit must compensate for a certain amount of electricity.



**Figure 8:** Thermal load operation optimization of the case 4

Combined with the optimization results of electricity and heat energy, Fig. 9 illustrates that EL is the primary hydrogen source within the EHRES system. The hydrogen produced by EL is primarily supplied to HFC, while the extra is stored within the HST. During the period of 22:00–6:00, when there is a surplus of wind power output, the price of electricity is at its lowest point; EL engages in high-power operations to convert the excess electric energy into hydrogen energy. Concerning heat load provision, HFC creates thermal energy to fulfill a portion of the heat load requirement, consequently diminishing carbon emissions and lowering the operational expenses of the system. During the time intervals of 6:00–10:00 and 16:00–21:00, the electric load is higher, the power of renewable energy is inadequate, the hydrogen production of EL is lower, and some hydrogen energy released by HST cannot meet HFC. Therefore, to meet the user’s electricity demand, CHP preferentially supplies electric power to satisfy the user’s need for electricity.

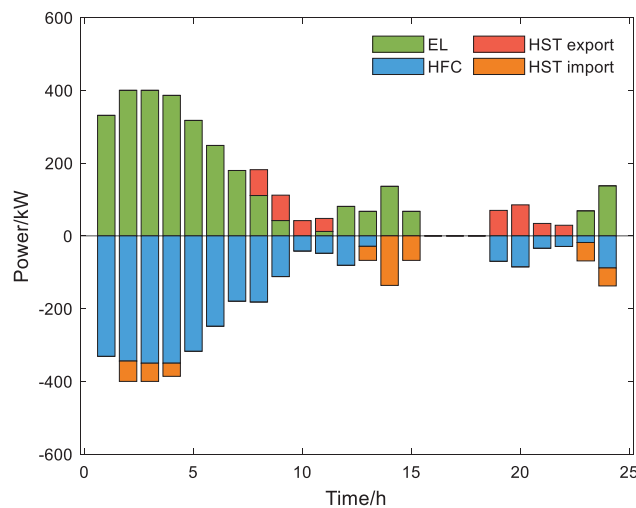


**Figure 9:** Hydrogen load operation optimization of the case 4

#### 4.2.4 System Sensitivity Analysis

The P2H system can store and supply multiple forms of energy simultaneously. The configuration of the P2H system in EHRES can effectively promote the interactive integration of various conversion devices. However, since China's current carbon trading price is constantly changing, its price change will have a meaningful impact on the P2H system configuration.

Fig. 10 illustrates a positive correlation between the carbon trading price and the power/capacity configuration of EL, HFC, and HST in the P2H system. With the carbon trading price increases, these components exhibit an upward trend in their configuration capacity. This suggests a preference for expanding their configuration capacity to facilitate low-carbon system scheduling. When the cost of carbon emissions surpasses 60 \$/t, the configuration of EL and HFC tends towards stability. In contrast, the HST's capacity demonstrates a heightened sensitivity to variations in carbon trading prices.

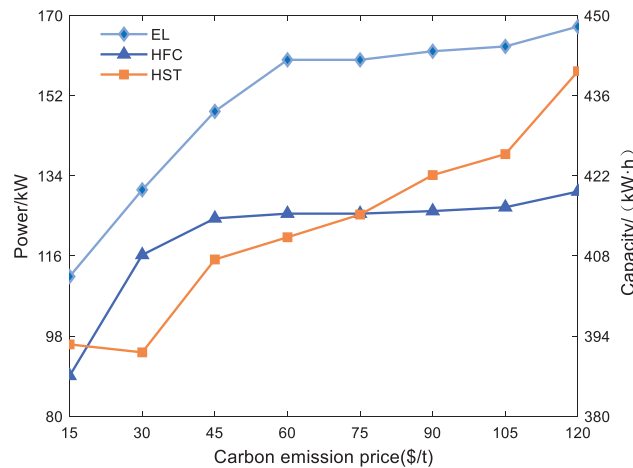


**Figure 10:** The configuration results of P2H system under different carbon trading prices

The economic benefits and carbon reduction benefits of participating in the carbon-electricity market transaction are influenced by variations in the storage capacity of HST. Hence, it is imperative to analyze HST's varying storage capacity to determine the impact on carbon trading costs and energy trading profits within the system.

Fig. 11 illustrates that when the capacity of the HST is below 140% of its initial capacity, any changes in its ability have minimal impact on the revenue generated by the electricity market. However, as the HST capacity continues to increase, there is a noticeable decline in revenue. Additionally, analyzing the carbon transaction cost reveals that as the HST hydrogen storage capacity increases, the carbon transaction cost generally follows a stepwise decrease pattern. Specifically, when the HST capacity is doubled, the system's income in the electric energy market decreases by 16.9%, and the cost of the carbon trading market decreases by 12.2%. Variations significantly influence the carbon transaction cost in hydrogen storage capacity. The increased capacity of the HST can effectively support the energy requirements of HFC cogeneration, resulting in more significant reductions in carbon emissions and decreased costs associated with carbon transactions within the system.

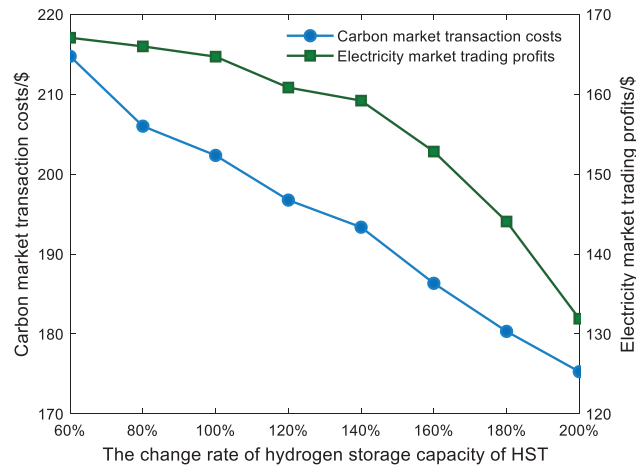


**Figure 11:** The influence of HST capacity on system operation benefit

Therefore, in determining the optimal capacity of the HST for the P2H system, it is essential to consider the augmented investment costs alongside the economic and carbon reduction benefits achievable within the carbon-electricity trading market. This assessment will assist in choosing the most appropriate HST capacity.

#### 4.2.5 Thermoelectric Ratio Analysis of HFC and CHP

Hydrogen energy itself has no carbon emissions. Incorporating HFCs into a combined heating system can lessen the system's reliance on high-carbon energy and increase its operational flexibility, making it better able to handle the peak-valley mismatch in thermoelectric load.

Fig. 12 illustrates that during the 1:00–4:00 period at night, there is a decrease in the electric load while the heat load reaches its highest point. The heat load is mainly supplied by HFC, showing a state of more heating and less power supply to maintain a higher thermoelectric ratio. During the 5:00–10:00 period, the CHP unit's heat output increases due to the gradual rise in electric demand and the gradual decline in heat load. This adjustment is made to sustain a higher thermoelectric ratio. Especially in the period of 16:00–23:00, there is a notable increase in electric and heat demands, resulting in a peak period. The lack of renewable energy production leads to the inefficiency of the EL, resulting in an inadequate hydrogen supply to HFC.

Consequently, the heat-to-electricity ratio of HFC is not taken into consideration. In general, HFC, as a new heat source, can supply heat to the thermal system by changing the heat-to-electricity ratio, providing 15.3% of the heat load during the heat-to-electricity conflict period of the CHP unit, thereby reducing the system's gas purchase cost. Since the hydrogen utilized in HFC primarily originates from EL, which is subject to the influence of renewable energy generation and fluctuations in load. The CHP unit can obtain a more stable gas supply from the upper gas network. Consequently, the CHP heat-to-electricity ratio curve shows a more stable trend than HFC.

From the analysis mentioned above, it is evident that taking into account the cogeneration characteristics of HFC can effectively facilitate the coordinated operation of electricity and heat, leading to a reduction in carbon emissions within the system. Consequently, the flexibility value of EHRES is further enhanced.

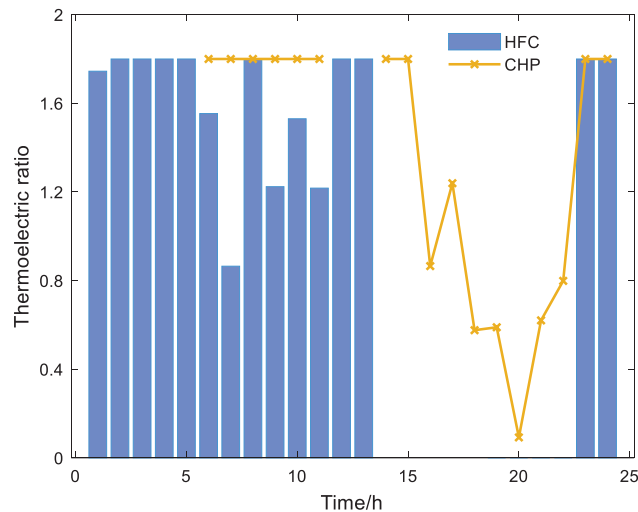


**Figure 12:** Optimization of combined heat and power generation characteristics of case 4

## 5 Conclusion

This study proposes an optimal operational strategy for EHRES that takes into account the attributes of HFC cogeneration in the context of carbon-electricity market transactions. The aim is to elevate the utilization rate of novel energy sources, curtail carbon emissions, and facilitate the achievement of the “double carbon” objective.

- By introducing the P2H system with HFC cogeneration characteristics, the electro-thermal coupling limitation of the traditional cogeneration unit can be further optimized, and the system’s capacity to reduce peak loads and fill in low-demand periods can be significantly enhanced. The system exhibits an improvement of 37.25% in electricity usage with the implementation of the P2H configuration. Additionally, there is an associated decrease in operating costs by 8.3%.
- Participation in carbon-electricity market transactions plays a crucial role in facilitating the achievement of emission reduction targets. The carbon reduction impact of the tiered carbon trading pricing system in the carbon-electricity market transaction is more substantial than the unified pricing mechanism. Through engagement in the carbon-electricity trading market, a reduction of 7.74% in carbon emissions is achieved for the scheduling cycle system. By comparing different schemes, this paper verifies the advantages of the proposed method under the carbon-electricity market transaction.
- The sensitivity analysis findings indicate a notable reduction in EHRES carbon emissions when the carbon price growth coefficient is increased, and the interval length is decreased. The capacity configuration of each piece of equipment inside the P2H system positively correlates with the carbon emission price growth. The variability in the hydrogen storage capacity of the HST has an impact on the system’s involvement in the transaction of carbon electricity in the market. Therefore, the rational allocation of the HST hydrogen storage capacity is conducive to reducing the system’s carbon transaction cost.

As P2H technology advances and undergoes extensive development in the future, realizing its full potential becomes crucial in boosting the utilization of renewable energy and fostering the growth of the green and low-carbon energy sector in the years ahead. In future research, we will delve deeper into the implications for the overall electricity market prices within the planning and operation

optimization of large-scale electro-hydrogen coupling systems. Additionally, we will explore investment optimization among different stakeholders, taking into consideration the uncertainties associated with renewable energy and related load characteristics. This will provide valuable insights to guide their investment decisions.

**Acknowledgement:** None.

**Funding Statement:** This work is supported financially by Inner Mongolia Key Lab of Electrical Power Conversion, Transmission, and Control under Grant IMEECTC2022001 and the S&T Major Project of Inner Mongolia Autonomous Region in China (2021ZD0040).

**Author Contributions:** The authors confirm contribution to the paper as follows: study conception and design: Jingyu Li, Mushui Wang, Na Zhang; data collection: Zhaoyuan Wu, Guizhen Tian; analysis and interpretation of results: Jingyu Li, Zhaoyuan Wu, Mushui Wang; draft manuscript preparation: Mushui Wang, Guangchen Liu. All authors reviewed the results and approved the final version of the manuscript.

**Availability of Data and Materials:** The authors confirm that the data supporting the findings of this study are available within the article.

**Conflicts of Interest:** The authors declare that they have no conflicts of interest to report regarding the present study.

## References

1. Wang, B., Li, L., Jiang, X. (2023). Sustainable development of energy systems and climate systems: Key issues and perspectives. *Energy Engineering*, 120(8), 1763–1773.
2. Yang, B., Guo, Z., Wang, J., Duan, C., Ren, Y. et al. (2022). Key optimization issues for renewable energy systems under carbon-peaking and carbon neutrality targets: Current states and perspectives. *Energy Engineering*, 119(5), 1789–1795.
3. Liu, T., Yang, Z., Duan, Y., Hu, S. (2022). Techno-economic assessment of hydrogen integrated into electrical/thermal energy storage in PV+ Wind system devoting to high reliability. *Energy Conversion and Management*, 268, 116067.
4. Morteza, Z., Hasan, M. (2022). Optimal allocation of power-to-hydrogen units in regional power grids for green hydrogen trading: Opportunities and barriers. *Journal of Cleaner Production*, 358, 131937.
5. Wang, J., An, Q., Zhao, Y., Pan, G., Song, J. et al. (2023). Role of electrolytic hydrogen in smart city decarbonization in China. *Applied Energy*, 336, 120699.
6. Burton, N., Padilla, R., Rose, A., Habibullah, H. (2020). Increasing the efficiency of hydrogen production from solar powered water electrolysis. *Renewable and Sustainable Energy Reviews*, 135, 110255.
7. Meng, X., Chen, M., Gu, A., Wu, X., Liu, B. et al. (2022). China's hydrogen development strategy in the context of double carbon targets. *Natural Gas Industry B*, 9, 521–547.
8. Rui, J., Hua, W., Lin, J., Lin, J., Zhao, Y. et al. (2022). Cost-efficient decarbonization of local energy systems by whole-system based design optimization. *Applied Energy*, 326, 119921.
9. Li, Y., Feng, T., Liu, L., Zhang, M. (2023). How do the electricity market and carbon market interact and achieve integrated development?—A bibliometric-based review. *Energy*, 265, 126308.
10. Wu, Q. (2022). Price and scale effects of China's carbon emission trading system pilots on emission reduction. *Journal of Environmental Management*, 314, 115054.

11. Li, Y., Sun, Y., Liu, J., Liu, C., Zhang, F. (2023). A data driven robust optimization model for scheduling near-zero carbon emission power plant considering the wind power output uncertainties and electricity-carbon market. *Energy*, 279, 128053.
12. Wang, S., Wang, S., Zhao, Q., Dong, S., Li, H. (2023). Optimal dispatch of integrated energy station considering carbon capture and hydrogen demand. *Energy*, 269, 126981.
13. Wang, J., Xue, K., Guo, Y., Ma, J., Zhou, X. et al. (2022). Multi-objective capacity programming and operation optimization of an integrated energy system considering hydrogen energy storage for collective energy communities. *Energy Conversion and Management*, 268, 116507.
14. Wang, Y., Liu, C., Qin, Y., Wang, Y., Dong, H. et al. (2022). Synergistic planning of an integrated energy system containing hydrogen storage with the coupled use of electric-thermal energy. *International Journal of Hydrogen Energy*, 48(40), 15154–15178.
15. Zeng, L., Wang, W., Zhang, W., Wang, Y., Tang, C. et al. (2023). Optimal configuration planning of vehicle sharing station-based electro-hydrogen micro-energy systems for transportation decarbonization. *Journal of Cleaner Production*, 387, 135906.
16. He, J., Wu, Y., Yong, X., Tan, Q., Liu, F. (2022). Bi-level optimization of a near-zero-emission integrated energy system considering electricity-hydrogen-gas nexus: A two-stage framework aiming at economic and environmental benefits. *Energy Conversion and Management*, 274, 116434.
17. Huang, C., Zong, Y., You, S., Træholt, C. (2022). Economic model predictive control for multi-energy system considering hydrogen-thermal-electric dynamics and waste heat recovery of MW-level alkaline electrolyzer. *Energy Conversion and Management*, 265, 115697.
18. Xiong, Y. F., Chen, L. J., Zheng, T. W., Yang, S., Mei, S. W. (2021). Electricity-heat-hydrogen modeling of hydrogen storage system considering off-design characteristics. *IEEE Access*, 9, 156768–156777.
19. Li, C., Zuo, X. (2022). Effects of hydrogen storage system and renewable energy sources for optimal bidding strategy in electricity market. *Energy Engineering*, 119(5), 1879–1903.
20. Fan, G., Liu, Z., Liu, X., Shi, Y., Wu, D. et al. (2022). Two-layer collaborative optimization for a renewable energy system combining electricity storage, hydrogen storage, and heat storage. *Energy*, 259, 125047.
21. Wang, J., Wu, Z., Du, E., Zhou, M., Li, G. et al. (2020). Constructing V2G-enabled regional energy internet toward cost-efficient carbon trading. *Journal of Power and Energy Systems*, 6(1), 31–40.
22. Liao, P., Liu, H., Wang, Y., Liao, N. (2023). Optimization of electricity purchase and sales strategies of electricity retailers under the condition of limited clean energy consumption. *Energy Engineering*, 120(3), 701–714.
23. Assaf, J., Shabani, B. (2018). Experimental study of a novel hybrid solar-thermal/pv-hydrogen system: Towards 100% renewable heat and power supply to standalone applications. *Energy*, 157, 862–876.
24. Lu, Z., Zhu, Q., Zhang, W., Lin, H. (2023). Economic operation strategy of integrated hydrogen energy system considering the uncertainty of PV power output. *Energy Reports*, 9(3), 463–471.
25. Yan, L., Liu, J., Ying, G., Zhang, N. (2023). Simulation analysis of flue gas waste heat utilization retrofit based on ORC system. *Energy Engineering*, 120(8), 1919–1938.
26. Wang, L., Dong, H., Lin, J., Zeng, M. (2022). Multi-objective optimal scheduling model with IGDT method of integrated energy system considering ladder-type carbon trading mechanism. *International Journal of Electrical Power & Energy Systems*, 143, 108386.
27. Lu, Q., Guo, Q., Zeng, W. (2021). Optimization scheduling of an integrated energy service system in community under the carbon trading mechanism: A model with reward-penalty and user satisfaction. *Journal of Cleaner Production*, 323, 129171.
28. Fan, G., Liu, Z., Liu, X., Shi, Y., Wu, D. et al. (2022). Energy management strategies and multi-objective optimization of a near-zero energy community energy supply system combined with hybrid energy storage. *Sustainable Cities and Society*, 83, 103970.

29. Akbari, S., Fazel, S. S., Hashemi-Dezaki, H. (2023). Energy management of networked smart railway stations considering regenerative braking, energy storage system, and photovoltaic units. *Energy Engineering*, 120(1), 69–86.
30. Ma, Y., Wang, H., Hong, F., Yang, J., Chen, Z. et al. (2021). Modeling and optimization of combined heat and power with power-to-gas and carbon capture system in integrated energy system. *Energy*, 236, 121392.
31. Teng, Y., Wang, Z., Li, Y., Ma, Q., Hui, Q. et al. (2023). Multi-energy storage system model based on electricity heat and hydrogen coordinated optimization for power grid flexibility. *CSEE Journal of Power and Energy Systems*, 5(2), 266–274.
32. Pan, G., Gu, W., Lu, Y., Qiu, H., Lu, S. et al. (2020). Optimal planning for electricity-hydrogen integrated energy system considering power to hydrogen and heat and seasonal storage. *IEEE Transactions on Sustainable Energy*, 11(4), 2662–2676.